Separation Science and Technology
Publication details, including instructions for authors and subscription information:
http://www.informaworld.com/smpp/title~content=t713708471

Structural Effects of Nanotubes, Nanowires, and Nanoporous Ti/TiO_2 Electrodes on Photoelectrocatalytic Oxidation of 4,4-Oxydianiline

Juliano Carvalho Cardoso[a]; Maria Valnice Boldrin Zanoni[a]
[a] Departamento de Química Analítica, Instituto de Química, Univ. Estadual Paulista, UNESP, Av. Prof. Francisco degni, Araraquara, SP, Brazil

Online publication date: 19 July 2010

To cite this Article Cardoso, Juliano Carvalho and Zanoni, Maria Valnice Boldrin(2010) 'Structural Effects of Nanotubes, Nanowires, and Nanoporous Ti/TiO_2 Electrodes on Photoelectrocatalytic Oxidation of 4,4-Oxydianiline', Separation Science and Technology, 45: 11, 1628 — 1636
To link to this Article: DOI: 10.1080/01496395.2010.487721
URL: http://dx.doi.org/10.1080/01496395.2010.487721

Separation Science and Technology, 45: 1628–1636, 2010

ISSN: 0149-6395 print/1520-5754 online
DOI: 10.1080/01496395.2010.487721

Taylor & Francis
Taylor & Francis Group

Structural Effects of Nanotubes, Nanowires, and Nanoporous Ti/TiO_2 Electrodes on Photoelectrocatalytic Oxidation of 4,4-Oxydianiline

Juliano Carvalho Cardoso and Maria Valnice Boldrin Zanoni
Departamento de Química Analítica, Instituto de Química, Univ. Estadual Paulista, UNESP, Av. Prof. Francisco degni, Araraquara, SP, Brazil

The present work illustrates the effect of electrolyte composition on the self-organized TiO_2 nanotube arrays electrode preparation. The influence of structural and surface morphology of the TiO_2 nanotube-like anode on their photoactivity and photoelectrocatalytic performance was also investigated. TiO_2 nanotubular array electrodes are grown by anodization of Ti foil in 0.25wt % NH_4F/glycerol/water, but nanowires can be obtained in 4% HF-DMSO as supporting electrolyte, even when both are subjected to electrochemical anodization at 30 V during 50 h. The morphological characteristics are analyzed by X-ray diffraction (XRD) and field emission scanning electron microscope (FEG-SEM). The electrodes were successfully applied in photoelectrocatalytic oxidation of 4,4′-oxydianiline (ODAN) in aqueous solution, as a model of a harmful pollutant. Complete removal of the aromatic amine was obtained after 3 hours of photoelectrocatalytic treatment on nanotubular arrays electrodes.

Keywords anodic oxidation; nanoporous electrode; nanowires film; TiO_2 nanotubes array

INTRODUCTION

Photoreactive materials have received much attention due to their inherent photochemical properties. Titanium dioxide (TiO_2) is a versatile semiconductor with a variety of applications in photocatalysis, gas sensors, photovoltaic cells, optical coatings, structural ceramics, and biocompatible materials (1,2). But, it is known from the literature (3) that the architecture of titania can greatly influence its physicochemical properties. Many techniques including sol-gel, precipitation–peptization, hydrothermal synthesis, and electrochemical methods have been developed to produce various nano-structured titania powders with good photoactivity (4–6), but the most popular method to immobilize TiO_2 films are those that use the dip-coating method. These films have shown great advances in photodegradation of organic pollutants (7–9). Nevertheless, the structural disorders, vast grain boundaries of the formed film are responsible for limited efficiency in the photoelectrocatalytic processes.

Titanium nanotubes, and nanotube arrays, have been investigated as alternative materials to improve the efficiency of photoeletrocatalytic technique. They can be produced by a variety of methods, including nanoporous template (7–10), hydrothermal processes (13–16), and by electrochemical growth (17–22).

Titania nanotube arrays can be easily grown by electrochemical anodization of titanium in fluoride-based baths by applying an electrical current between a Ti electrode and a counterelectrode. Typically the tube diameter is controlled by the applied anodization voltage (23–25) and the length can be varied by means of the anodization time and by using different electrolytes containing fluoride ions. Anodization under constant-voltage conditions leads to an ordered layer consisting of a distinct morphology of smooth tubes with defined cylindrical or hexagonal cross section (26–27).

The formation of nanotube arrays in a fluoride containing electrolyte is the result of three simultaneously occurring processes:

1. field assisted oxidation of Ti metal to form titanium dioxide,
2. field assisted dissolution of Ti metal ions in the electrolyte, and
3. chemical dissolution of Ti and TiO_2 due to etching by fluoride ions (25).

In general, it appears that the key to successfully achieving very long titania nanotube arrays using polar organic electrolytes is to minimize the water content to less than 5% (26). With organic electrolytes the donation of oxygen is more difficult in comparison to water and results in a reduced tendency to form oxide (27), while the reduction in the water content allows for thinner or lower quality barrier layers through which ionic transport may be enhanced.

Received 3 November 2009; accepted 3 March 2010.
Address correspondence to Maria Valnice Boldrin Zanoni, Departamento de Química Analítica, Instituto de Quimica, University for São Paulo State, UNESP, C.P. 355, Araraquara, SP 14801-970, Brazil. E-mail: boldrinv@iq.unesp.br

The aim of the present work was to investigate the effect of parameters such as: time anodization, applied potential, annealed temperature, and electrolyte composition on the self-organized TiO_2 nanotube arrays electrode preparation. The influence of structural and surface morphology of the TiO_2 nanotube-like anode on their photoactivity is also studied. The electrodes were applied in photoelectrooxidation of 4,4′-oxydianiline (ODAN) in aqueous solution, as a model of a harmful pollutant in order to optimize a treatment method for wastewater containing carcinogenic amine. ODAN is an aromatic amine that can enter the aqueous environment via the reduction of azo dyes and nitroaromatic compounds and are an important class of anthropogenic chemical (28) with mutagenic/carcinogenic activity. In addition, the performance of nanotube arrays electrodes is compared with titanium-supported titania photoelectrodes made by sol-gel techniques. The ODAN degradation kinetics parameters have been evaluated through total organic carbon (TOC) removal, spectrophotometric and chromatographic analysis to assess the effectiveness of the photoelectrocatalytic oxidation method.

MATERIALS AND METHODS

Preparation of TiO_2 Nanotubes and Nanowires by Anodization Methods

The titanium foils (99.95%, Alfa Aesar) were 0.25 mm thick with a geometric area of 25 cm^2. They were polished to a mirror quality smooth finish using silicon carbide sandpaper of successively finer roughness (220, 320, 400, 500, 1200, and 1500 grit) and degreased by successively sonicating for 15 min in isopropanol, acetone, and finally ultrapure water. They were then dried under a flowing N_2 stream and used immediately.

Highly ordered TiO_2 nanotube arrays were prepared by a potentiostatic anodization in a two-electrode electrochemical cell. A titanium foil with a size of 5 cm × 5 cm was used as a working electrode, and a platinum foil with a size of 2 cm × 2 cm served as a counterelectrode. The interval between the working electrode and counterelectrode was about 1 cm. The voltage was applied by a DC power supply (model MQ of Microquímica, Brazil). The TiO_2 nanotube array and TiO_2 nanowires were formed by anodizing the Ti foil in 150 mL of organic electrolyte, which showed a dependence on the anodization time. The present organic electrolytes were 0.25% ammonium fluoride (97.0%, Fisher) in glycerol (98.5%, Fisher) containing 10% volume Milli-Q water for the formation of nanotubes arrays and DMSO (Sinth) and fluoridic acid 10% (40%, Nuclear) for the formation of nanowires. For both methods, the electrodes were annealed at 450°C for 30 min in a furnace (model 650–14 Isotemp Programmable Muffle Furnace, Fisher Scientific) and were allowed to cool gradually back to the ambient condition.

Preparation of TiO_2 Nanoporous by Sol Gel Method

Titanium (IV) isopropoxide (Aldrich) was used as a precursor for preparing TiO_2 colloidal suspensions. Typically, 20 mL of titanium isopropoxide was added to a nitric acid solution keeping the ratio of $Ti/H^+/H_2O$ at 1/1.5/200. The resulting precipitate was continuously stirred until completely peptized to a stable colloidal suspension. This suspension was dialyzed against ultrapure water (Milli-Q Millipore) to a pH of 3.5 using a Micropore 3500 MW membrane. Thin-film photoelectrodes with geometric area of 25 cm^2 were obtained after dip-coating of a titanium-foil backed contact (0.05 or 0.5 mm thick, and 5.0 × 5.0 cm – Goodfellow Cambridge Ltd.) after previous cleaning and heating to 450°C during 30 min. A sequence of dipping, drying, and annealing at 450°C for 3 h was used after each coating (four repetitions) according to a procedure described earlier (7).

Characterization Technique

The morphologies of all samples were examined using a JEOL JSM-6300 field emission scanning electron microscope (FEG-SEM) of LME-LNLS, Sincroton, Campinas-SP. The crystalline phases were detected and identified by a glancing angle X-ray diffractometer Rigaku RINT 1500 X-ray diffraction meter using Cu KR radiation in the range of 20–60°. The surface chemical composition of samples was analyzed by X-ray photoelectron spectroscopy (XPS) from Kratos Analytical Axis Ultra. Monochromatic aluminum (1486.6 eV) was used as the X-ray source (280 W). All binding energies were calibrated to C−C C1s peak at 285 eV of the surface adventitious carbon. For studies of the photocatalytic properties and for measurement of photoeletrocatalytic degradation, a Potentiostat/Galvanostat Autolab model 302 was used.

Degradation Experiments

Photoelectrocatalytic, photocatalytic, and direct photolysis were performed in a 250 mL photoelectrochemical reactor equipped with water refrigeration using an ultra thermosthatic bath (Nova Técnica, Brazil). The cell was equipped with a working electrode, an auxiliary electrode, Pt gauze, and Ag/AgCl (KCl, 3 M) reference electrode. The photoactive area of the TiO_2 nanotube arrays, nanowires, and nanoparticles were 25 cm^2 and it was illuminated with UV-A light source (315–400 nm) using a 125 W Philips medium pressure mercury lamp ($I = 9.23\ W\ m^{-2}$) without the glass, inserted in a quartz bulb. All experiments were carried out using sodium sulfate 0.1 $mol L^{-1}$ at pH 2, as supporting electrolyte. Initial concentration of ODAN was $5.0 \times 10^{-6}\ mol\ L^{-1}$. Photocatalytic experiments were carried out using electrodes without polarization and UV-A light. The direct photolysis of ODAN measurements were conducted only in the presence of UV-A light. An

applied potential of 1.5 V vs Ag/AgCl under UV-A irradiation was used for the photoelectrocatalytic oxidation.

Spectroscopy, Organic Carbon, and Chromatographic Analysis

Absorption spectra in the ultraviolet and visible range were recorded with a Hewlett-Packard spectrophotometer, model HP 8452A in a 10 mm quartz cell. Total organic carbon analyzer (TOC-V_{CPN}, Shimadzu, Japan) was employed for the mineralization degree analysis of ODAN solution. Prior to injection into the TOC analyzer, the samples were filtrated with 0.45 μm Millipore filter to remove any particles. A high performance liquid chromatograph Model Shimadzu 10 AVP coupled with a diode array detector was used to separate the products and intermediates generates. A column separation C-18 (4.6 mm × 250 mm, 5 mm) and mobile phase methanol/phosphate buffer (50:50 (v/v)) with a flow of 1.0 mL min^{-1} were used. The chromatographic signals from the peaks were analyzed by integration of the area. The aromatic amine peak was monitored in 244 nm. The procedures were performed in triplicate for each sample.

RESULTS AND DISCUSSION

Morphological Characteristics of Thin Film TiO_2 Electrodes

The formation of TiO_2 nanotube arrays on the surface of titanium was investigated using two methods: Ti foil was inserted in a solution of

a. glycerol/water/NH_4F (90%/10%/0.25% v/v) and
b. DMSO/HF 4% (v/v).

They were submitted to voltage application of 20 V or 30 V during time anodization of 5, 20, and 50 hours, followed by 30 min of calcinations at a temperature of 350°C and 450°C.

FEG-SEM images obtained for the samples prepared in the 0.25% NH_4F in Glycerol – Water solution grown during 50 hours at 30 V, annealed at 450°C are illustrated in Fig. 1, images A, B, and C. The top view FEG-SEM micrographs of the TiO_2/Ti nanotubes clearly show that the surface morphology of the samples is characterized by an extended open porous network of highly ordered nanotubes (C) in different magnifications. The cross-sectional images indicate that the nanotube arrays are highly ordered and perpendicular (B) to the titanium substrate, which data are shown in Table 1. Self-assembly of nanotubular TiO_2 arrays are seen on films of the Ti surface obtained by all anodization conditions tested. But the lengths of the nanotube arrays increased with the anodization time, while the small diameter is obtained with lower anodization potential.

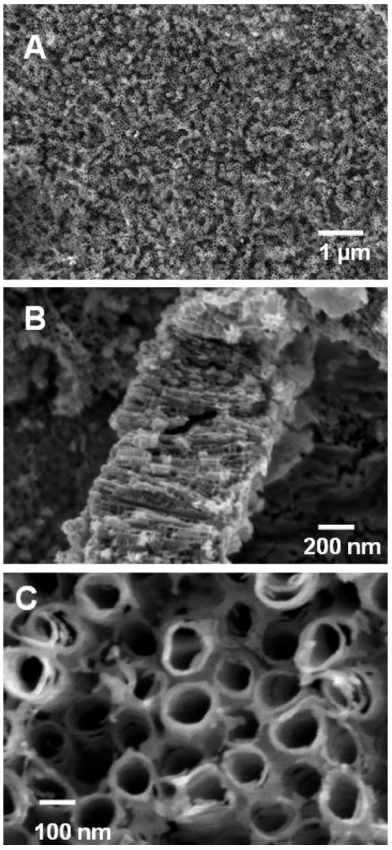

FIG. 1. SEM images of the TiO_2 nanotube layer formed in glycerol + water (90:10%) respectively and 0.25% NH_4F at 30 V for 50 hours and annealed to 450°C: (A,C) Top view; (B) cross-sectional images.

Figure 2 (Graphs A, B, and C) shows the FEG-SEM images obtained in solution of 4% HF-DMSO as supporting electrolyte during 50 hours at 30 V, annealed at 450°C. In this electrolyte is clearly observed the formation of a structural disorder of the film of TiO_2 assigned as nanowires. Values of length and diameters of formed nanowires are shown in Table 1. The nanowires dimensions are experimental dependent on conditions. In HF concentrations higher than 2.0% films of TiO_2 present shorter nanowires with thinner walls. Therefore, the architecture of the nanotube arrays in self-organized TiO_2 nanotube arrays

TABLE 1
Anodization conditions and respective size of the yielding nanotubes, nanowires and nanoparticles films

Sample	T(°C)	E(V)	t (hours)	D(nm)	L (nm)
Nanotubes	450	30	50	101 ± 8	1073 ± 53
Nano wires	450	30	50	40 ± 4.5	3000 ± 80
Nanoparticles	450	30	–	20 ± 6	–

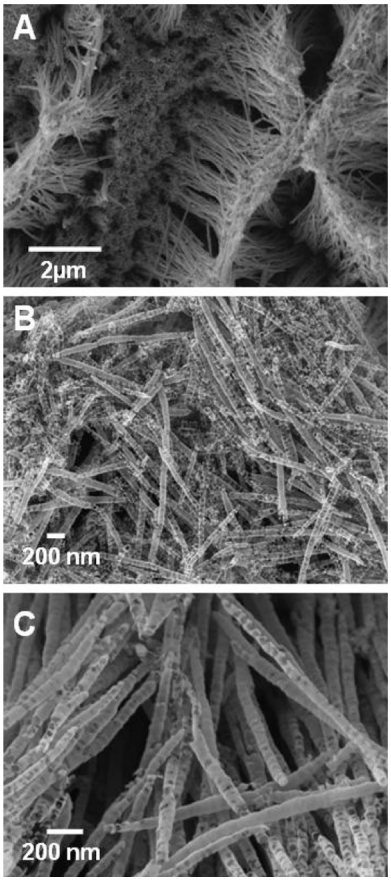

FIG. 2. SEM images of the TiO_2 nanowires layer formed in DMSO +4% HF at 30 V for 50 hours and annealed to 450°C, (A–C) Top views.

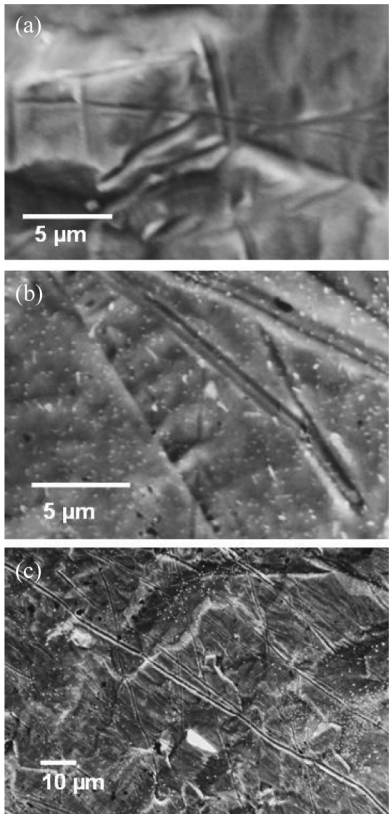

FIG. 3. SEM images of the nanoporous TiO_2 layer prepared by sol-gel procedure and annealed to 450°C, (a–c) Top views.

seems more dependent of electrolyte than the applied potential or the anodization time (29,30).

Figures 3 (a–c) illustrate the FEG-SEM images of samples of TiO_2 films produced as nanoparticle material by the sol-gel process, annealed at 450°C. The entire surface is coated with TiO_2 nanoparticle on the order of 10 until 20 nm. The grain analysis indicates that they are uniformly compacted and dispersed on the film surface. Nanostructured films are formed with homogeneous geometry and compact arrangement.

A factor that is expected to affect markedly the electronic properties of the nanotubes walls is the crystal structure of TiO_2 (2). Figure 4 shows a comparison of X-ray diffraction (XRD) patterns of nanotubes (Fig. 4d), nanowires (Fig. 4c) of TiO_2 samples obtained after 50 h at 30 V, as mentioned previously and nanoparticles electrodes of TiO_2 (Curve B, Fig. 4) submitted to annealing at 450°C and electrodes without calcination (Curve A, Fig. 4). Results indicate that the as-fabricated samples (A) TiO_2 films are amorphous and the presence of rutile allotropic forms ($2\theta = 27.7$) is neglected on the films, but a defined peak of the anatase phase ($2\theta = 25$) is observed for both nanotubes and nanowires films. From the relative intensity of both peaks at $2\theta = 27.7$, and 25, it is possible to notice that anatase forms is 5.4 times higher in nanotube composition in relation to the nanowires electrode and 52 times in relation to the nanoparticles electrodes.

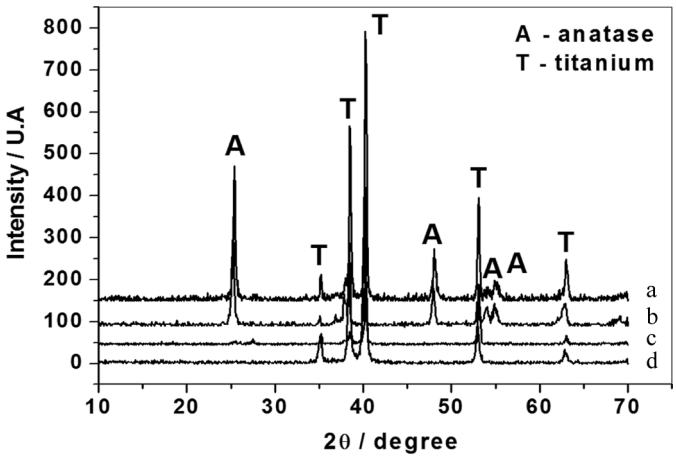

FIG. 4. XRD patterns of samples (a) before annealed; (b) nanoporous TiO_2; (c) nanowires TiO_2 and (d) nanotube arrays TiO_2 annealed to 450°C.

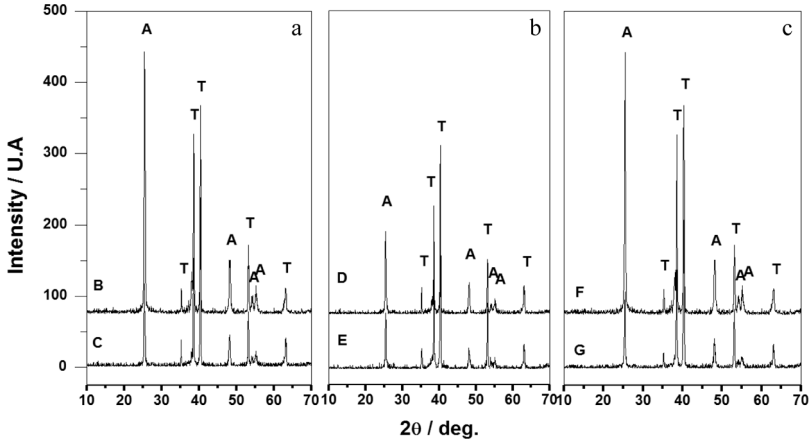

FIG. 5. XRD patterns of samples ((A) change of the time (B = 50 and C = 20 hours)), ((B) change of potential (D = 30 and E = 20 V)) and ((C) change of temperature (F = 450 and (G) 350°C)).

For nanotube arrays TiO_2 films, the diffraction peaks of anatase form are all enhanced by the increased length of nanotube arrays and higher annealing temperature, as shown in Fig. 5. The peak of anatase form in the electrode composition is around 3.1 times higher for electrode prepared at 50 hours in relation to that obtained at 20 h (Fig. 5a). The XRD pattern of the long nanotube arrays contains a neglected rutile peak at 27.7° and the anatase form is 1.7 times higher for films prepared at applied potential of 30 V than 20 V (Fig. 5b). It is also 3.4 times higher in electrodes annealed at 450°C than that prepared at temperature of 350°C (Fig. 5c). As expected the TiO_2 nanotubes presents a mixture of anatase and rutile forms in its composition when annealed at temperatures close to 450°C (31–34). Thus, it is possible to conclude that the choice of electrolyte has no influence on the crystalline structure of the resultant oxide films (2), but the others parameters, such as applied voltage, anodization time, and annealing temperature can markedly affect the characteristic of the yielding material of thin film TiO_2.

TiO_2 nanotubular array (NTA) electrodes, grown by anodization of Ti foil in 0.25 wt% NH_4F and a mixture of glycerol and water (ratio 90:10 vol%) using an applied voltage of 30 V for 50 h. In order to determine the elemental composition of the nanotube, nanowires, and nanoporous samples, X-ray photoelectron spectroscopy (XPS) analysis was conducted and the results obtained are summarized in Table 2. The samples are predominately titanium and oxygen, with traces of fluorine due to solvent incorporation in the film. The source for the nitrogen and carbon found in the samples could be attributed to surface contamination. Chemical-state analysis for titaniun indicates the sample is Ti^{4+} bonded with oxygen (TiO_2) for both samples. Hence, while the results of XPS and XRD indicate that a considerable amount of solvent is trapped in the amorphous anodic films, the trapped elements such as F and C do not enter into the anatase or rutile lattice.

TABLE 2
XPS results of samples TiO_2 prepared by using of different process. Annealing temperature = 450°C, Annealing time 30 min

	Atomic concentration (%)				
	Ti	O	F	N	C
Nanotubes	28.3	64.5	0.8	0.5	5.1
Nanowires	21.4	55.1	0.8	–	6.2
Nanoporous	25.8	74.1	–	0.2	6.5

Photoactivity of Ti/TiO_2 Thin Films Electrodes

The photoactivity properties of the thin films TiO_2/Ti electrodes were analyzed by recording a set of linear sweep voltammograms with and without UV illumination using three different anodes: (A) nanowires Ti/TiO_2 electrode; (B) nanotubular Ti/TiO_2 electrode array and (C) nanoparticles Ti/TiO_2 electrode in 0.1 molL^{-1} Na_2SO_4 solution. The analytical results as photocurrent vs potential curves are presented in Fig. 6.

The voltammetric curves of Ti/TiO_2 electrodes under UV illumination (curves B, C, and D) demonstrated the response of the anodic current appearing above −0.25 V vs Ag/AgCl for all anodes nanoparticles (B), nanotubes (C), and nanowires (D) electrodes. Nevertheless, the nanoporous Ti/TiO_2 electrodes exhibited the lower current response than the nanotubular array and nanowires TiO_2/Ti electrodes.

The photocurrent density taken at applied potential of 1.5 V indicates that the nanotubular array Ti/TiO_2 electrode (Fig. 6c) was 10 times more intense than the nanoporous Ti/TiO_2 electrode (Fig. 6b), which is also

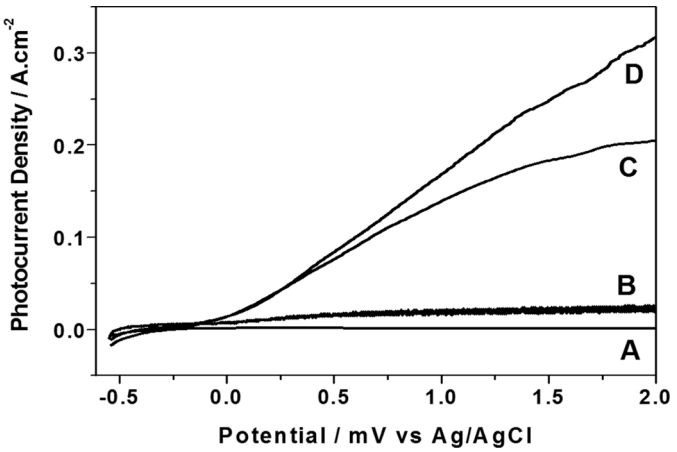

FIG. 6. Photocurrent density versus applied potential (vs Ag/AgCl) in 0.1 molL^{-1} Na_2SO_4 solution. (A) Dark current for each sample; (B) nanoporous TiO_2 prepared by sol-gel procedure; (C) TiO_2 nanotube arrays prepared by anodization at 30 V during 50 hours in glycerol + water + NH_4F mixture solution and (D) TiO_2 nanowires formed in DMSO + 4% HF at 30 V during 50 hours. Both samples were annealed at 450°C for 30 min in oxygen atmosphere prior to testing.

approximately 2 times less intense than nanowires Ti/TiO_2 electrode (Fig. 6d). The yielding response of anodic currents in the photocatalytic experiment is a combination of photocurrent and an electrochemical current. While the electrochemical current results from the water oxidation on the Ti/TiO_2 anode activated by UV irradiation, the photocurrent should result from a regular transfer of TiO_2 conduction band electrons excited by UV irradiation. It is well known (2) that the most photo-induced electron/hole pairs (e^-/h^+) could be recombined quickly, although TiO_2 electrons can be easily excited from the valence band to the conduction band by UV excitation. In such a photoelectrochemical reaction system, the externally applied anodic potential on the Ti/TiO_2 electrode could drive the photo-induced electrons from the TiO_2 conduction band to form an external circuit current and enhance the $e^-/h+$ separation. However, the overall efficiency of electron transfer through a Ti/TiO_2 electrode depends highly on the surface micro-structure of TiO_2 films and its supporting material. Their can be influences on the electron transition inside the semiconductor and electron-transfer on the interface of the TiO_2/Ti electrode (34). Apparently, the experimental results in this study demonstrate that higher photocurrent response occurred when the applied potential was above 1.5 V vs Ag/AgCl. However, to avoid significant anodic corrosion (or dissolution) of the TiO_2/Ti electrode itself, the potential applied was controlled to a maximum of 1.5 V vs Ag/AgCl.

Under UV irradiation the anodic current increased very slowly at the low voltage range and increases continuously over a critical oxidation potential of water due to oxygen evolution. When this electrolyzing voltage was further increased above the critical oxidation potential of Ti, a sharp enhancement of anodic current occurred, resulting from a titanium metal oxidation reaction along with a water-splitting reaction. The curve A of TiO_2/Ti electrodes in the dark showed that their critical dielectric breakdown potentials were about 3 V. This result demonstrated a typical character of n-type semiconductor, where a large anodic current only occurs over a breakdown potential. Obviously, this anodic current of the TiO_2/Ti electrode should be derived from not only the reaction of oxygen evolution, but also anodic dissolution of the TiO_2 electrode itself. However, the latter effect plays an insignificant role when the applied potential is below the electric breakdown potentials of the Ti/TiO_2 electrode. This phenomenon is different from that of the Ti metal electrode.

Performance of Nanotube, Nanowire, and Nanoparticles Ti/TiO_2 Electrodes on Photoelectrocatalytic Degradation of 4,4-Oxydianiline

The primary role of an electrocatalyst for photooxidation processes is to provide very low valence band edge energy, E_{VB}, and to make the surface electrons–holes to act as powerful oxidizing sites for generating radical oxidants in reactions with the medium. In order to test its efficiency in photoelectrocatalytic oxidation, experiments were carried out testing the nanotubes array, nanowires, and nanoparticule Ti/TiO_2 electrodes on the degradation of 4,4-oxydianiline (ODAN) in 0.1 molL^{-1} Na_2SO_4 pH 2.0, as a model compound of harmful pollutant demanding high levels of removal. The bias potential values applied on all experiments conducted under UV irradiation were 1.5 V vs Ag/AgCl. The degradation of ODAN was followed by measurements of absorbance of ODAN that presents a characteristic absorbance at $\lambda = 244$ nm and 300 nm assigned to an aromatic ring and R-NH_2 groups, observed from the UV-Visible absorption spectra. The degradation of ODAN was monitored taking maxima absorbance values at 244 nm. The experiments were also monitored by HPLC with a diode array detector, where ODAN presents a high defined peak at a retention time of 4.5 minutes, using the optimum conditions previously investigated and TOC measurements to follow mineralization.

The results obtained from UV spectra indicates that 2 hours of photoelectrocatalytic treatment of ODAN reaches 96% removal on nanotubes electrodes (Fig. 7a, Graphic A) while the nanowires and nanoparticles electrodes reach 92 and 85% after 3 hours as shown in Fig. 7a, Graphs B and C, respectively. Analysis carried out by HPLC confirmed the reduction of the concentration of ODAN after 30 minutes of photoelectrocatalytic treatment using three electrodes (Fig. 7b, Graphic A–C). The kinetics constants obtained for ODAN photoelectrocatalytic oxidation on nanotubes, nanowires, and nanoparticule film of TiO_2

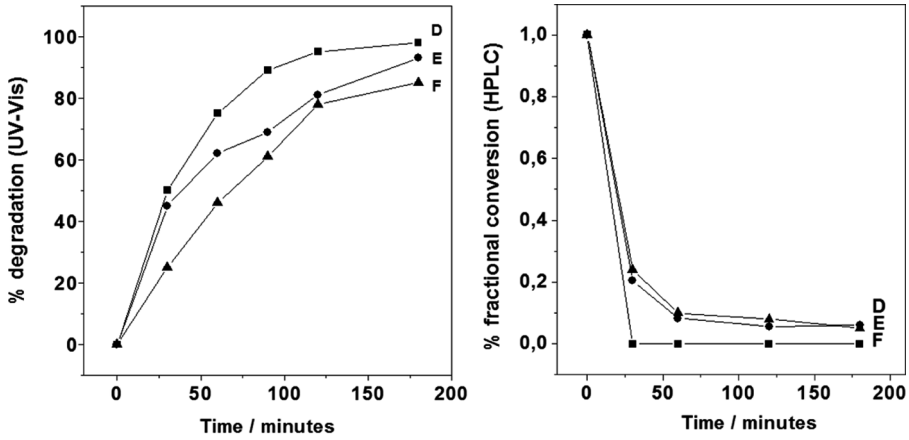

FIG. 7. HPLC-DAD obtained before (A) and during degradation of ODAN by PEC (B) on: nanotube arrays (D); nanowires (E) and nanoporous TiO_2 electrodes (F).

electrodes present a linear relationship of ln $[A_t/A_0]$ *vs* time, where A_t is the absorbance at time (t) and A_0 is the absorbance at zero time, suggesting a mechanism following a pseudo-first-order. The degradation rate constant are $0.0196\,min^{-1}$ ($R = 0.998$ and $SD = 0.025$), $0.0151\,min^{-1}$ ($R = 0.997$ and SD 0.0201), and $0.0115\,min^{-1}$($R = 0.996$ and SD 0.019) for ODAN photoelectrocatalytic oxidation on nanotubes, nanowires, and nanoparticulated film of TiO_2 electrodes. These results suggest that the photoelectrocatalytic activity on the nanotube array TiO_2 electrode was higher than that of the TiO_2 nanowires and nanoparticule film electrodes.

This behavior is also confirmed by TOC removal monitoring photoelectrocatalytic oxidation of 5.0×10^{-6} $molL^{-1}$ of ODAN. A maximum of mineralization follows the order: 99% on nanotube array TiO_2 electrode, 87% on TiO_2 nanowires, and 76% TiO_2 film electrode after 3 h of treatment, as shown in Fig. 8. This result illustrates the potentiality of the nanotubes electrodes in relation to other electrodes. This behavior could be attributed to the favorable electron transport and high superficial area in nanotube arrays and is further supported by the enhanced anodic photocurrent response compared with nanoparticulate film obtained by sol-gel. But, the advantage of nanotubes in relation to nanowires electrodes is an example of how the ordered structural deposit of TiO_2 arrays are very favorable for the transport of the photogenerated electrons in the TiO_2 film, which is vital in the photoelectrocatalytic oxidation process. Taking into account that the photoelectrocatalytic oxidation of ODAN is powered mainly by hydroxyl radicals, which is generated from the trapping of the photogenerated holes by the water or the hydroxyl on the surface of TiO_2, the lifetime of the holes on the surface of TiO_2 is a preponderant process to the degradation of the pollutant. The present nanotube array is perpendicular to the substrate and has a continuous architecture from the surface to the substrate. In addition, these characteristics can also interfere in the adsorption/desorption of the dye on the electrode surface (35,36). Irradiated by UV light, the applied positive bias can drive the photogenerated electrons in a unidirectional channel to transport quickly to the counterelectrode, which increases the lifetime of photogenerated holes and improves the degradation rate of the aromatic amine, as verified previously for phenol degradation (3). The grain boundaries occurrence in the nanoparticles and nanowires electrodes and the convoluted channels for electron transport increase the competition of charge recombination, resulting in lower photoelectrocatalytic activity.

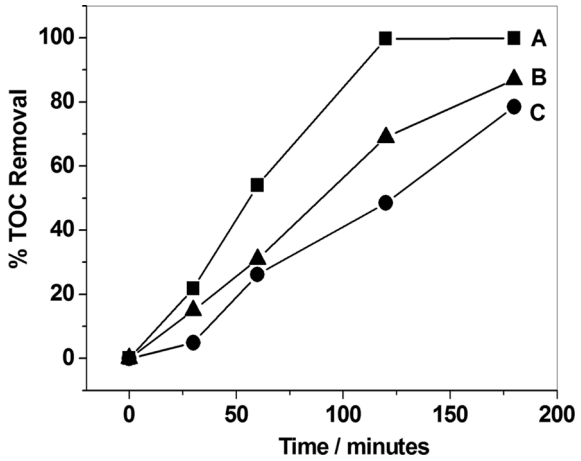

FIG. 8. Influence of the electrodes (A) nanotubes; (B) nanowires and (C) nanoporous TiO_2 in the photoelectrocatalytic degradation of aromatic amine ODAN ($5.0 \times 10^{-6}\,molL^{-1}$) in $0.1\,molL^{-1}$ Na_2SO_4 pH 2.0 and bias potential of 1.5 V.

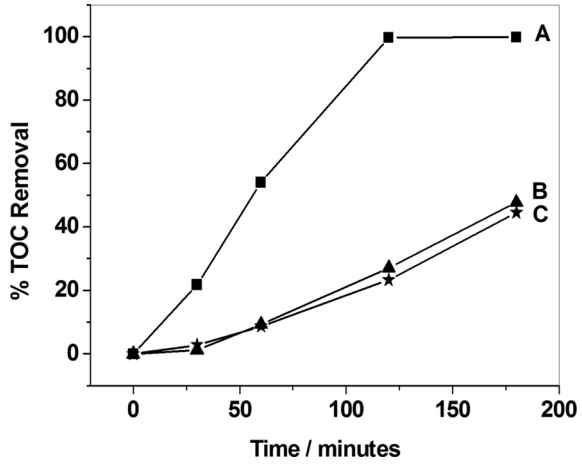

FIG. 9. Mineralization of aromatic amine ODAN by photoelectrocatalytic (PEC), photocatalysis (PC) and photolysis (DP) processes process on: (A) PEC – nanotubes; (B) PC – nanotubes and (C) DP. Time of treatment = 180 min. ODAN concentration = 5.0×10^{-6} molL^{-1} in 0.1 molL^{-1} Na_2SO_4 pH 2.0. Bias potential = 1.5 V.

Comparison of PEC, Photocatalysis and Direct Photolysis for ODAN Degradation

Experiments on photoelectrocatalysis (PEC), photocatalysis (PC), and direct photolysis (DP) mineralization of ODAN were carried out in order to compare ODAN mineralization efficiencies. For this the three individual processes were carried out by measuring its mineralization on nanotubes arrays of TiO_2 anode, as shown in Fig. 9. Direct UV irradiation (DP) promoted 37% of ODAN mineralization in 3 hours. By using the photocatalytic process the nanotubes arrays of TiO_2 (without bias supply) mineralized 43% of the ODAN during the same time. Nevertheless, the process is markedly improved under an applied potential of 1.5 V, reaching 99% of the ODAN mineralization after 2 hours of photoelectrocatalytic treatment.

CONCLUSIONS

Our findings illustrate that self- organized TiO_2 nanotubular array electrodes can be easily obtained by using anodic oxidation of Ti in organic and viscous electrolytes, which present higher photoactivity than nanoporous film of Ti/TiO_2 prepared by the sol-gel method. The use of high dielectric constant organic solvent allows a larger potential window for nanotube formation and enhances the rate of migration of the metal/oxide interface into the substrate. By control of the electrolyte, potential and anodization time, it is possible to obtain an ordered structure of the nanotubes, with preponderant anatase from in the composition, and higher photocurrent magnitude than a compact film. The effect is highest for higher potential than the flat band potential. At higher anodic voltages this strong effect diminishes due to geometric constraints of the nanotubes, i.e., the space change layers generated at both sides of the nanotubes fills essentially the entire pore wall width. These materials can be a good strategy to treat effluents containing aromatic amine. The use of nanotube arrays of TiO_2 as electrode presented a higher efficiency to promote ODAN degradation than on nanowires and nanoporous electrodes. Degradation and mineralization of ODAN was faster by the photoelectrocatalysis process than photocatalysis or direct photolysis.

ACKNOWLEDGEMENTS

The authors acknowledge the financial support provided by the Brazilian funding agency FAPESP process 2007/07313-3; LME-LNLS, Campinas, Brazil, for the use of FEG-SEM.

REFERENCES

1. Fujishima, A.; Rao, T.N.; Tryk, D.A. (2000) TiO_2 photocatalysts and diamond electrodes. *Electrochimica ACTA*, 45 (28): 4683–4690.
2. Gratzel, M. (2001) Photoelectrochemical cells. *Nature*, 414 (6861): 338–344.
3. Liu, Z.; Zhang, X.; Nishimoto, S.; Jin, M.; Tryk, D.A.; Murakami, T.; Fujishima, A. (2008) Highly ordered TiO_2 nanotube arrays with controllable length for photoelectrocatalytic degradation of phenol. *J. Phys. Chem. C*, 112 (1): 253–259.
4. Arabatzis, I.M.; Antonaraki, S.; Stergiopoulos, T.; Hiskia, A.; Papaconstantinou, E.; Bernard, M.C.; Falaras, P. (2002) Preparation, characterization and photocatalytic activity of nanocrystalline thin film TiO_2 catalysts towards 3,5-dichlorophenol degradation. *J. Photochem. Photobiol. A-Chem.*, 149 (1–3): 237–245.
5. Reddy, G.R.; Lavanya, A.; Anjaneyulu, C. (2004) Effect of current density on the anodic behaviour of zircaloy-4 and niobium: A comparative study. *Bull. Electrochem.*, 20 (8): 337–341.
6. Hore, S.; Palomares, E.; Smit, H.; Bakker, N.J.; Comte, P.; Liska, P.; Thampi, K.R.; Kroon, J.M.; Hinsch, A.; Durrant, J.R. (2005) Acid versus base peptization of mesoporous nanocrystalline TiO_2 films: functional studies in dye sensitized solar cells. *J. Mater. Chem.*, 15 (3): 412–418.
7. Zanoni, M.B.; Sene, J.J.; Anderson, M.A. (2003) Photoelectrocatalytic degradation of Remazol Brilliant Orange 3R on titanium dioxide thin-film electrodes. *J. Photochem. Photobiol. A: Chem.*, 157 (1): 55–63.
8. Osugi, M.E.; Rajeshwar, K.; Oliveira, D.P.; Araujo, A.R.; Ferraz, E.R.; Zanoni, M.V.B. (2009) Comparison of oxidation efficiency of disperse dyes by chemical and photoelectrocatalytic chlorination and removal of mutagenic activity. *Electrochim. Acta*, 54 (7): 2086–2093.
9. Carneiro, P.A.; Osugi, M.E.; Sene, J.J.; Anderson, M.A.; Zanoni, M.V.B. (2004) Evaluation of color removal and degradation of a reactive textile azo dye on nanoporous TiO_2 thin-film electrodes. *Electrochim. Acta.*, 49 (22–23): 3807–3820.
10. Hoyer, P. (1996) Formation of a titanium dioxide nanotube array. *Langmuir*, 12 (6): 1411–1413.
11. Lakshmi, B.B.; Dorhout, P.K.; Martin, C.R. (1997) Sol-gel template synthesis of semiconductor nanostructures. *Chem. Mater.*, 9 (3): 857–862.
12. Imai, H.; Takei, Y.; Shimizu, K.; Matsuda, M.; Hirashima, H. (1999) Direct preparation of anatase TiO_2 nanotubes in porous alumina membranes. *J. Mater. Chem.*, 9 (12): 2971–2972.
13. Michailowski, A.; AlMawlwai, D.; Cheng, G.S.; Moskovits, M. (2001) Highly regular anatase nanotubule arrays fabricated in porous anodic templates. *Chem. Phys. Lett.*, 349 (1,2): 1–5.

14. Jung, J.H.; Kobayashi, H.; Van Bommel, K.J.C.; Shinkai, S.; Shimizu, T. (2002) Creation of novel helical ribbon and double-layered nanotube TiO_2 structures using an organogel template. *Chem. Mater.*, 14 (4): 1445–1447.
15. Kobayashi, S.; Hamasaki, N.; Suzuki, M.; Kimura, M.; Shirai, H.; Hanabusa, K. (2002) Preparation of helical transition-metal oxide tubes using organogelators as structure-directing agents. *J. Am. Chem. Soc.*, 124 (23): 6550.
16. Tian, Z.R.R.; Voigt, J.A.; Liu, J.; McKenzie, B.; Xu, H.F. (2003) Large oriented arrays and continuous films of TiO_2-based nanotubes. *J. Am. Chem. Soc.*, 125 (41): 12384–12385.
17. Kasuga, T.; Hiramatsu, M.; Hoson, A.; Sekino, T.; Niihara, K. (1998) Formation of titanium oxide nanotube. *Langmuir*, 14 (12): 3160–3163.
18. Osugi, M.E.; Zanoni, M.V.B.; Chenthamarakshan, C.R.; Tacconi, N.R. de; Wondemariam, G.A.; Mandal, S.S.; Rajeshwar, K. (2008) Toxicity assessment and degradation of disperse azo dyes by photoelectrocatalytic oxidation on Ti/TiO_2 nanotubular array electrodes. *J. Adv. Oxid. Technol.*, 11 (3): 425–434.
19. de Tacconi, N.R.; Chenthamarakshan, C.R.; Yogeeswaran, G.; Watcharenwong, A.; de Zoysa, R.S.; Basit, N.A.; Rajeshwar, K. (2006) Nanoporous TiO_2 and WO_3 films by anodization of titanium and tungsten substrates: influence of process variables on morphology and photoelectrochemical response. *J. Phys. Chem. B*, 110 (50): 25347–25355.
20. Mor, G.K.; Varghese, O.K.; Paulose, M.; Shankar, K.; Grimes, C.A. (2006) A review on highly ordered, vertically oriented TiO_2 nanotube arrays: Fabrication, material properties, and solar energy applications. *Sol. Energy Mater. Sol. Cells.*, 90 (14): 2075.
21. Bauer, S.; Kleber, S.; Schmuki, P. (2006) TiO_2 nanotubes: Tailoring the geometry in H_3PO_4/HF electrolytes. *Electrochem. Commun.*, 8 (8): 1321–1325.
22. Tsuchiya, H.; Macak, J.M.; Ghicov, A.; Schmuki, P. (2006) Self-organization of anodic nanotubes on two size scales. *Small*, 2 (7): 888–891.
23. Albu, S.P.; Ghicov, A.; Macak, J.M.; Schmuki, P. (2007) 250 μm long anodic TiO_2 nanotubes with hexagonal self-ordering. *Phys. Status Solidi RRL*, 1 (2): R65–R67.
24. Macak, J.M.; Albu, S.P.; Schmuki, P. (2007) Towards ideal hexagonal self-ordering of TiO_2 nanotubes. *Phys. Status Solidi RRL*, 1 (5): 181–183.
25. Mor, G.K.; Varghese, O.K.; Paulose, M.; Mukherjee, N.; Grimes, C.A. (2003) Fabrication of tapered, conical-shaped titania nanotubes. *J. Mater. Res.*, 18 (11): 2588–2593.
26. Paulose, M.; Shankar, K.; Yoriya, S.; Prakasam, H.E.; Varghese, O.K.; Mor, G.K.; Latempa, T.A.; Fitzgerald, A.; Grimes, C.A. (2006) Anodic growth of highly ordered TiO_2 nanotube arrays to 134 μm in length. *J. Phys. Chem. B*, 110 (33): 16179–16184.
27. Foll, H.; Langa, S.; Carstensen, J.; Christophersen, M.; Tiginyanu, I.M. (2003) Pores in III-V semiconductors. *Adv. Mater.*, 15 (3): 183–198.
28. IARC 1987, Overall Evaluations of Carcinogenicity, IARC Monographs on the Evaluation of Carcinogenic Risk of Chemical to Humans, Supplement 7, International Agency for Research on Cancer, Lyon, France.
29. Albu, S.P.; Kim, D.; Schmuki, P. (2008). Growth of aligned TiO_2 bamboo-type nanotubes and Highly ordered nanolace. *Electrochemical Nanotechnology.*, (47): 1916–1919.
30. Kim, D.; Ghicov, A.; Albu, S.P.; Schmuki, P. (2006). Bamboo-type TiO_2 nanotubes: Improved conversion efficiency in dye-sensitized solar cell. *J. Am. Chem. Soc.*, (130): 16454–16455.
31. Varghese, O.K.; Gong, D.; Paulose, M.; Grimes, C.A.; Dickey, E.C. (2003) Crystallization and high-temperature structural stability of titanium oxide nanotube arrays. *Journal of Materials Research.*, 18 (1): 156–165.
32. Ghicov, A.; Tsuchiya, H.; Macak, J.M.; Schmuki, P. (2006) Annealing effects on the photoresponse of TiO_2 nanotubes. *Phys Stat Sol A.*, 203 (4): R28–R30.
33. Macak, J.M.; Aldabergerova, S.; Ghicov, A.; Schmuki, P. (2006) Smooth anodic TiO_2 nanotubes: annealing and structure. *Phys Stat Sol A.*, 203 (10): R67–R69.
34. Zhao, J.; Wang, X.; Sun, T.; Li, L. (2005) In situ templated synthesis of anatase single-crystal nanotube arrays. *Nanotechnology*, 16 (10): 2450–2454.
35. Stergiopoulos, T.; Valota, A.; Likodimo, V.; Speliotis, Th.; Niarchos, D.; Skeldon, P.; Thompson, G.E.; Falaras, P. (2009) Dye-sensitization of self-assembled titania nanotubes prepared by galvanostatic anodization of Ti sputtered on conductive glass. *Nanotechnology*, 20: 365601–9.
36. Alexaki, N.; Stergiopoulos, T.; Kontos, A.G.; Tsoukleris, D.S.; Katsoulidis, A.P.; Pomonis, P.J.; LeClere, D.J.; Skeldon, P.; Thompson, G.E.; Falaras, P. (2009) Mesoporous titania nanocrystals prepared using hexadecylamine surfactant template: Crystallization progress monitoring, morphological characterization and application in dye-sensitized solar cells. *Microporous and Mesoporous Materials*, 124: 52–58.